

PAPER • OPEN ACCESS

A study on intermediate buffer layer of coated Fiber Bragg Grating cryogenic temperature sensors

To cite this article: R Freitas *et al* 2015 *IOP Conf. Ser.: Mater. Sci. Eng.* **101** 012154

View the [article online](#) for updates and enhancements.

Related content

- [Observation of depolarized guided acoustic-wave Brillouin scattering in partially uncoated optical fibers](#)
Neisei Hayashi, Sze Yun Set and Shinji Yamashita
- [Chemical beam epitaxy of GaN on Si \(111\)](#)
T S Huang, T B Joyce, R T Murray *et al.*
- [Preparation of \$\text{Bi}_4\text{Ti}_3\text{O}_{12}/\text{Bi}_2\text{SiO}_5/\text{Si}\$ Structures Derived by Metal Organic Decomposition Technique](#)
Masaki Yamaguchi, Takao Nagatomo and Yoichiro Masuda

Recent citations

- [Metallic-packaging fiber Bragg grating sensor based on ultrasonic welding for strain-insensitive temperature measurement](#)
Lianqing Zhu *et al*
- [Experimental investigation on mass flow rate measurements using fibre Bragg grating sensors](#)
S. R. Thekkethil *et al*
- [Numerical and experimental investigation of FBG strain response at cryogenic temperatures](#)
V. N. Venkatesan and R. Ramalingam



IOP | ebooks™

Bringing you innovative digital publishing with leading voices to create your essential collection of books in STEM research.

Start exploring the collection - download the first chapter of every title for free.

A study on intermediate buffer layer of coated Fiber Bragg Grating cryogenic temperature sensors

R Freitas¹, F Araujo², J Araujo¹, H Neumann³, and R Ramalingam³

¹Department of Physics and Astronomy, University of Porto, 4099-002 Porto, Portugal

²FiberSensing, Rua Vasconcelos Costa 277, 4470-640 Maia, Portugal

³Institute of Technical Physics (ITEP), Karlsruhe Institute of Technology (CN), P.O. Box 3640, D-76021, Karlsruhe, Germany

E-mail: rajini-kumar.ramalingam@kit.edu

Abstract. The sensor characteristics of a coated Fiber Bragg grating (FBG) thermal sensor for cryogenic temperatures depends mainly on the coating materials. The sensitivity of the coated FBG can be improved by enhancing the effective thermal strain transfer between the different layers and the bare FBG. The dual coated FBG's has a primary layer and the secondary layer. The primary coating acts as an intermediate buffer between the secondary coating and the bare FBG. The outer secondary coating is normally made of metals with high thermal expansion coefficient. In this work, a detailed study is carried out on chromium and titanium intermediate buffer layers with various coating thicknesses and combinations. To improve the sensitivity, the secondary coating layer was tested with Indium, Lead and Tin. The sensors were then calibrated in a cryogenic temperature calibration facility at Institute of Technical Physics (ITEP), Karlsruhe Institute of Technology. The sensors were subjected to several thermal cycles between 4.2 and 80 K to study the sensor performance and its thermal characteristics. The sensor exhibits a Bragg wavelength shift of 13pm at 20K. The commercially available detection equipment with a resolution of 1pm can result in a temperature resolution of 0.076 K at 20K.

1. Introduction

Selection of right sensors and an appropriate measurement system has become a challenging task as the operational requirements of the new technologies demands to measure extreme temperatures and conditions. The physical properties of the sensing material can change drastically in extreme temperatures. This is particularly true in the case of cryogenic applications where decreasing the temperature to near absolute zero alters the behaviour of materials. Their crystal structures become more compact and the lattice vibrations tend to cease, since the thermal energy is not enough to excite phonons. The temperature at which this change of behaviour occurs is known as the "Debye Temperature" and is a characteristic of each material.

In the most advanced research centers, such as those using large particle accelerators [1], where cryogenic temperatures are essential for the proper operation of sensitive equipment, sensors capable of operating in these temperature ranges are essential. They serve to monitor both the conditions of a complex set of equipments required to perform the experiments, and to ensure the safety of the equipment itself.



In order to fulfil the increasing demand for suitable cryo temperature sensors needed in advanced applications like ITER, KATRIN [2], HTS Geno [3], the researchers look into the optical fiber sensors, which show distinctive advantages like immunity to electromagnetic interference and power fluctuations along the optical path, high precision, durability, compact size, ease of multiplexing a large number of sensors along a single fiber, resistance to corrosion and reduced cable dimensions [4-7]. Among many optical fiber sensing techniques, Fiber Bragg Grating (FBGs) has become very prominent sensing method for many applications [8 – 12] and are being increasingly accepted by engineers, as they are particularly attractive to perform strain and temperature measurements under harsh environment areas, where conventional sensors cannot operate [13].

Moreover, the fact that it is stimulated by light signal minimizes the power dissipation in the sample while offering accuracy well suited to most applications. The response time is potentially low given the smaller sensor-size. Also the conditioning of the spectral signal can be easily processed with commercially available equipment.

These capabilities make this type of sensors a preferable solution for monitoring environments where high electromagnetic fields are needed, such as those associated with monitoring of infrastructures used in superconducting magnets. When electrical sensors are used, the thermal conductivity of the signal wires (4 wires per measuring site) as well as magneto-resistance and parasitic voltages induced in strong magnetic fields are common problems which are difficult to mitigate. For example, it is already well known [14] that conventional resistance strain gauges (RSG) show increasing discontinuities in their strain-dependent electric resistance with decreasing temperature (between 20 K and 4.2 K). Also standard, low temperature sensors, for example, Si-diodes or resistors are influenced by magnetic fields. [15].

Many groups are actively involved in designing and fabricating FBG sensors and studying its thermal characteristics. It was shown experimentally that the Bragg wavelength of fused silica fibers with Germanium doped core becomes independent of temperature below 120 K. This is beneficial for structural health monitoring (strain) in cryogenic systems. On the other hand, bare fibers with FBG cannot be used for temperature measurements below 120 K. To overcome this problem, several solutions were proposed. Fixing the FBG on a substrate that shows a high thermal expansion such as polymer [16], flint-glass [17] or metals [18] result in a temperature dependence of several pm/K. Alternatively, metal-coating [19] of the fibers also lead to a measurable temperature dependence of the Bragg wavelength with minimal time lag.

Proper selection of coating materials and the coating techniques determine the performance and characteristic of a metal coated optical cryo sensor. When selecting a coating material one should consider the 3 main factors which contribute greatly in transferring thermal strain in the grating element. They are *Coefficient of thermal expansion (CTE)*, *Young's modulus (E)*, and *Adhesion*.

In order to obtain sensitivity at very low temperatures the coating material must have expansion/contraction at those temperatures. If that doesn't happen in the temperature range of interest then that material should be discarded as a prospective coating material. Hence, the coefficient of thermal expansion is the most important coating material's characteristic. The Young's modulus is the second most important characteristic of the coating material. Even if the chosen material has high CTE, it still needs to have enough strength to overpower the bare grating in its own expansion behaviour. If this wouldn't happen the sensor would have a negligible improvement when compared to the bare grating.

Adhesion is the third parameter of extreme importance, for even if the two parameters above are met but the coating shows poor adhesion to the grating its impact on the sensitivity would be reduced and could cause the improved sensitivity to disappear after a few cycles. If a coating material with good CTE and E shows poor adhesion to the grating a buffer layer should be used between them. This buffer should have minimal dimensions when compared to the fiber's diameter and coating while presenting good adhesion between both.

In this paper, the sensor performance of the chromium and titanium intermediate buffer / primary coating layer with various thicknesses and combinations has been studied. The metals like lead, indium and tin has been used as a secondary layer.

2. Coating intermediate buffer / primary layer

Electron beam deposition (EBD) technique was used to do the buffer depositions after verifying its capability to deposit thin films with high homogeneity. The films deposited were 100 to 200 nm thick and made of Titanium, Chromium and Nickel. The electron beam deposition device was modified to suit the fiber coating needs. Figure 1 and 2 shows the modified device which allows for homogeneous and simultaneous deposition of materials on six fibers which are rotating at a constant speed inside the vacuum chamber.



Figure 1. Opened EBD chamber used for thin film deposition of the buffer layers on the FBGs.

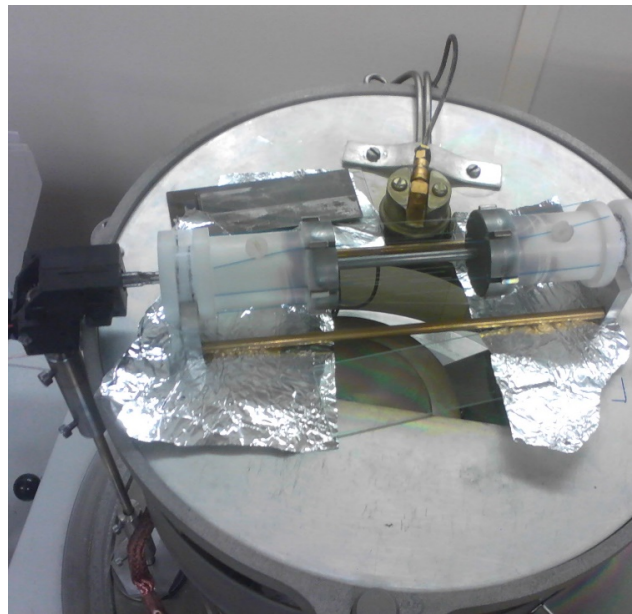


Figure 2. Apparatus that allowed for the homogeneous thin film deposition on multiple fibers.

The films deposited were 100 to 200 nm thick and made of Titanium, Chromium and Nickel. In order to do this deposition, initially the fibers were placed on the rotating device and the setup was kept inside the vacuum chamber. A vacuum of 10^{-7} mbar was achieved inside the chamber in 3 hours. Then the fiber was kept rotating at the rate of 6.6 rpm. This rotation ensures the uniform deposition of metals all around the fiber. The metals were deposited at the rate of ~ 0.03 nm/s. Due to the fact that the metals used had high melting points and that the energy dissipated in the form of heat inside the chamber was also high, the deposition had to be paused for around 1 hour. This means that the device had to be paused after every 30 to 40 minutes. To produce 100 nm film it took nearly 3 hours with 1 pause and for 200 nm film it took nearly 6 hours with 3 to 4 intervals.

Deposition tests were made on several fibers and on glass substrates in order to test their adhesion. These were cleaned with water, alcohol and acetone on a Quimwipe paper, and then dipped in liquid nitrogen no peeling of the films was observed.

A Scanning Electron Microscope (SEM) was used on one of these fibers deposited with a 100nm thin film of Chromium. In the SEM images from Figure 3 it is possible to see that apart from some debris the film described above is very homogenous and presents no cracks or peeling. The EBD was established to be a very good deposition technique; Titanium and Chromium were proven to have good adhesion to the fiber.

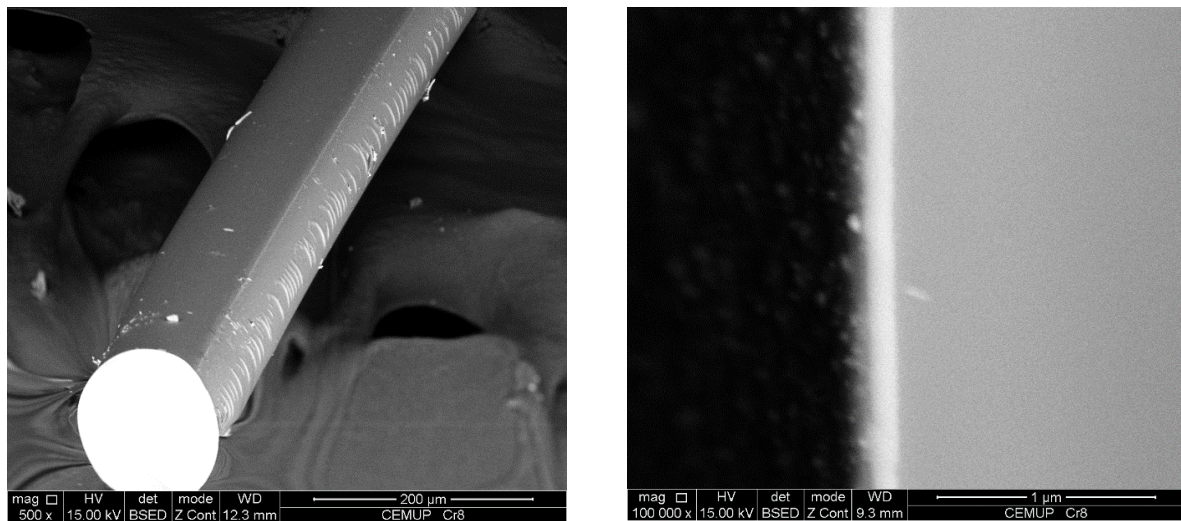


Figure 3. SEM analysis of an optical fiber partially coated with a 100nm Cr thin film.

3. Coating outer / secondary layer

Electron Beam Deposition however, do not allow for a good deposition of thick films of around 500 microns which was the thickness intended for the outer / secondary layers. The fact that this is a Physical Vapor Deposition (PVD) does not allow for all the atoms to be chemically bound together resulting in grains for thicker films. Another disadvantage is that for high thickness, this technique is too time and power consuming. In order to fabricate sensor with a thick secondary layer faster, and to conduct the initial test regarding the buffer layer, it was decided to use the casting method for secondary layer preparation. This technique was considered a valid alternative since the temperatures required do not affect the fiber or the thin films. Also, in order to attenuate the low homogeneity at the sensor's surface the casting mold to be used would have a diameter at least 15 times the diameter of the fiber.

A mold was made of CERNIT, a thermal insulating polymer easily moldable where the shape of a small cylinder was imprinted, as well as a channel for the optical fiber, in order for it to be centered with the cylinder. Magnetic clamps were used to hold the fiber in place. This apparatus is shown in Figures 4 and 5. The CERNIT mold underwent a 30 minute annealing at 393K where it lost its malleability and became rigid.

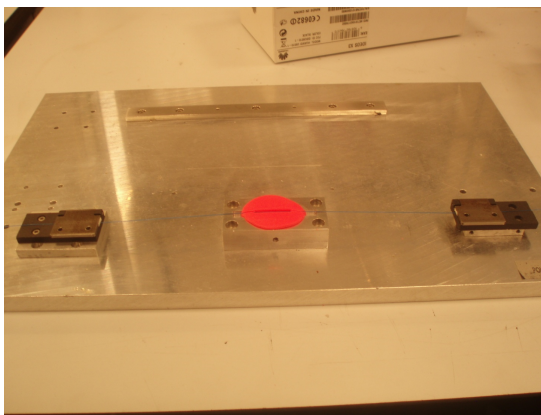


Figure 4. Apparatus used for the sensor construction.

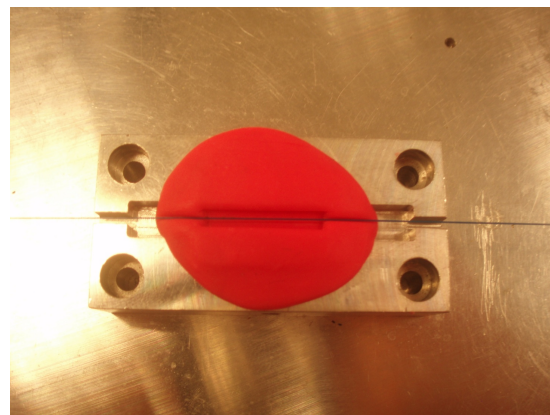


Figure 5. Mold used for the sensor construction.

An optical fiber with a FBG was placed on the mold ensuring that the grating was inside the cylindrical impression. The gratings used were previously coated with 200nm of Titanium or Chromium, using Ebeam deposition. Using temperature controlled soldering iron small pieces of the metal in study were melted until the cavity was filled. After ensuring the grating was inside, the metal the assembly was left to cool. This cavity was approximately 15mm long and 2.5mm in diameter.

During this process the fiber containing the FBG was connected to a FS 2200- 8 channel BraggMETER and the spectrum was monitored for changes which helped ensure that there were no tensions on the grating before it was left to cool.

Table 1. Sensors fabricated with different buffer and secondary layer.

Series	Thin Film Coating	External Coating
S1, S2	100 nm Ti	In , Pb
S3, S4	200 nm Ti	In, Pb
S5,S6	100 nm Cr	In, Pb
S7, S8	200 nm Cr	In, Pb
S9, S 10	50 nm Cr + 50 nm Ni	In , Pb
S11 , S12	150 nm Cr + 18.5 nm Ni	In, Pb

The films with Cr + Ni were inserted in this study because according with [20] Ni has a good adhesion to In and Ni has a good adhesion to Cr.

4. Experimental setup and conduction

Among the fabricated sensors, 32 sensors of good quality with different buffer and secondary coating layers were spliced together to form a 4 sensor array with 8 sensors in each array. Care has been taken to ensure that the sensor in each array had a different resonant wavelength. These sensor arrays were then placed inside cylindrical holes in a calibration block made of copper. The sensors were held inside the calibration block using polystyrene foam. A Class B calibrated thin film PT-1000 temperature was used as reference sensor, which was also inserted in the center of the calibration block. The entire setup was then inserted inside a cryostat and the optical and electrical communication devices, BraggMETER and the DMM was connected via the optical and electrical feedthroughs respectively. The pressure gauges were also installed on the top of the flange of the cryostat that would allow the monitoring inside pressure. The calibration block and the cryostat can be seen in Figures 6 and 7.

The cryostat was then closed and connected to a He recovering system existing in the facility for He recycling. The cryostat was initially filled with liquid nitrogen to cool the system down to 77 K and then the supply of Liquid helium was started to cool the system down to 10 K. The response of the FBG sensor array and the PT 1000 sensor was recorded simultaneously. Warming up was done by natural convection to atmosphere.

A total of nine thermal cycles were done between 4.2 and 80K to anneal the FBG sensor behaviour in this thermal region, to remove internal stresses existing in the coating materials and to study the thermal characteristics at this temperature range. The sensor behaviour was found to be drifting for the first six cycles, but in the last three cycles the thermal behaviour of the sensor has become stable and repeatable for all sensing arrays except for the chromium buffer layer. These results infer that the metal coated FBG sensor may need temperature training for at least 10 cycles to make a meaningful reliable measurement.

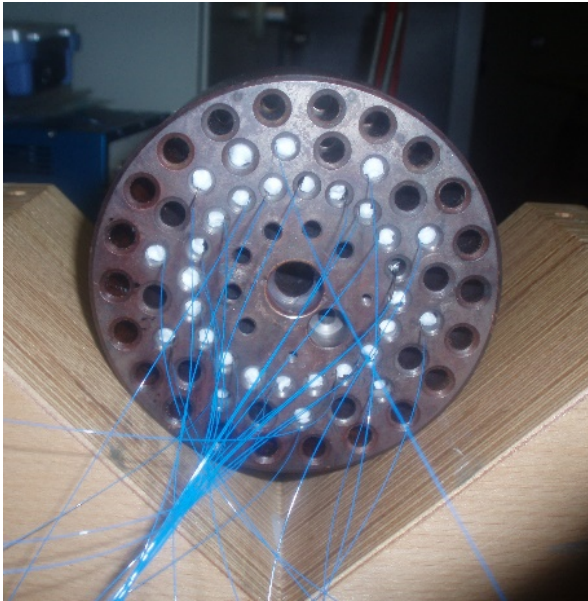


Figure 6. Copper block used for cryogenic temperature tests containing all FBG sensors constructed.



Figure 7. Cryostat used for the first tests with all FBG sensors.

Figures 8, 9 & 10 show the wavelength shifts of three sensors with different buffers and with Indium secondary layers. It can be observed from figure 8 that the sensor initially shows a repeatable characteristic for cycle 7 and 8, but then the 9th cycle was again showing a great drift of about 10 % from the previous cycles. This shows that the adhesion of the chromium buffer layer between the fiber and the indium secondary layer is not enough. When a Nickel layer is added between the chromium and Indium, then the sensor shows highly repeatable performance with an error of less than 2 % only.

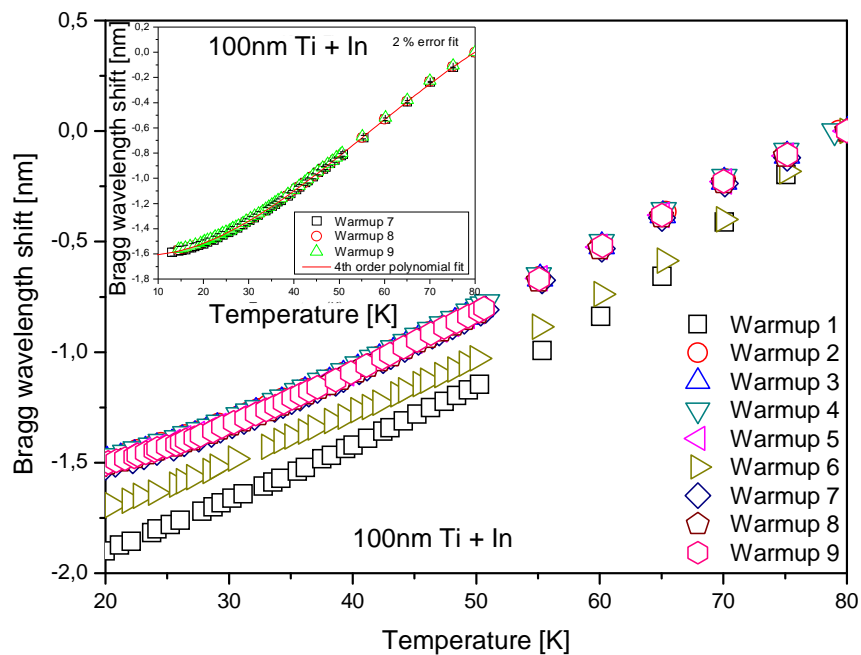


Figure 8. Sensor 1B 100nmTi+In wavelength shift during warm-ups for all nine cycles and then only for the last three showing repeatability.

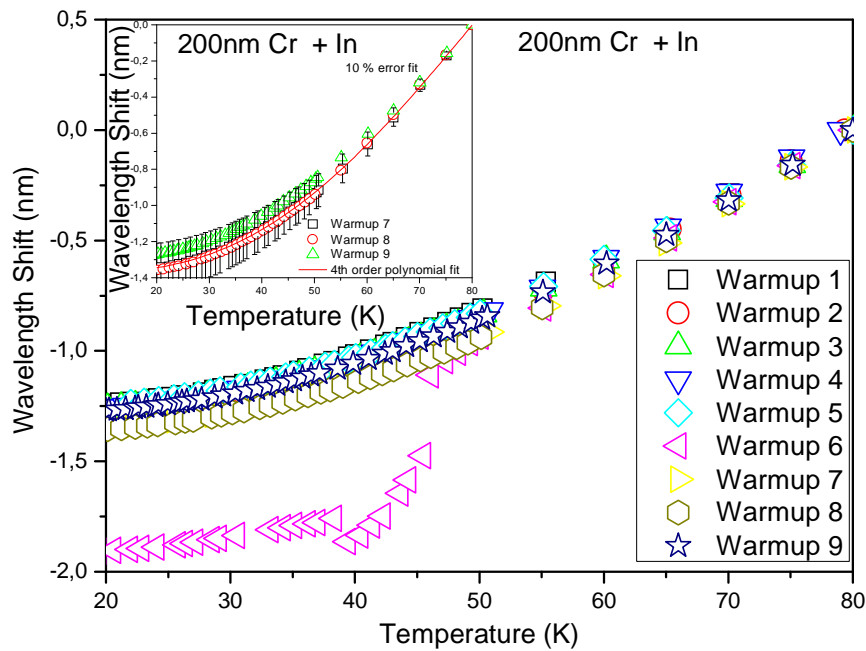


Figure 9. Sensor 4 B 200nmCr+In wavelength shift during warm-ups for all nine cycles and then only for the last three showing repeatability.

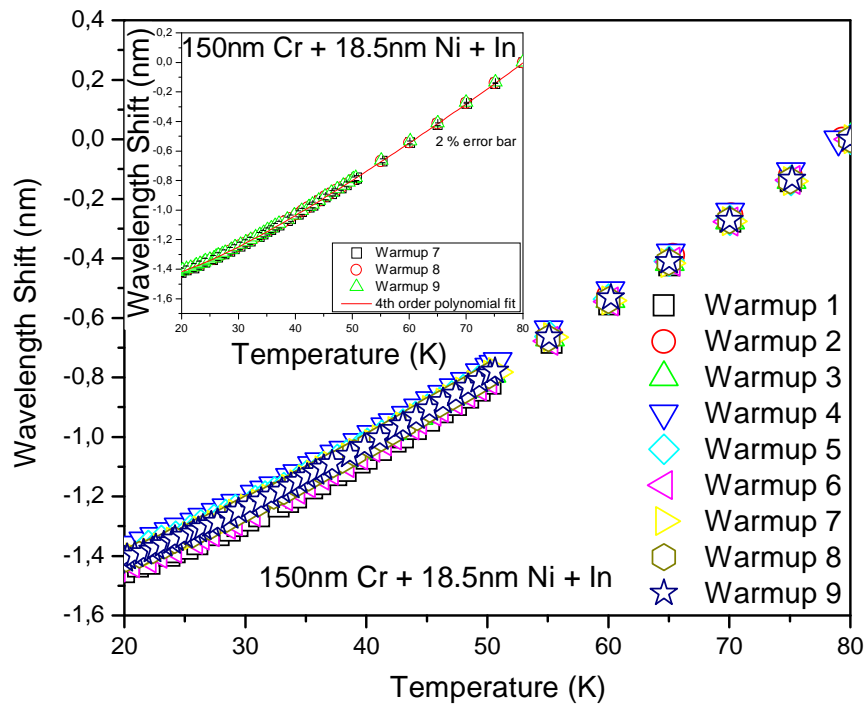


Figure 10. Sensor 1G 150nmCr+18.5nmNi+In wavelength shift during warm-ups for all nine cycles and then only for the last three showing repeatability.

The graphs of the last three warm-ups of each sensor were used to determine these sensor temperature sensitivities giving special attention to the temperature range between 20 and 40K. It has been estimated that the temperature sensitivity of the fabricated sensors was found to be 34 pm/K at

40 K and 13pm/ K at 20 K. With the available commercial Bragg meter (FS 2200) this translates into the temperature resolution of 0.29 K and 0.76 K respectively.

Table 2. Sensitivity of sensors fabricated with different buffer and secondary layer for the temperature range of (20-40) K

Temp	Sensitivity pm/K												
	S1	S2	S3	S4	S5	S6	S7	S8	S9	S10	S11	S12	
	1B	4A	4H	3H	5E	Broken	4B	3C	4E	4D	1G	Broken	
20K	13	12	10	13	5		13	7	14	13	13		
30K	18	19	15	19	10		18	8	19	17	17		
40K	34	34	29	35	25		34	14	30	35	29		
Buffer	100nmTi		200nmTi		100nmCr	200nmCr		50nmCr+		150nmCr+		50nmNi	18.5nmNi

5. Conclusion

In this work, the temperature characteristics of FBG sensors with titanium, chromium and chromium plus nickel buffer layers were studied. The sensors fabricated with different buffer layers were then coated with indium and lead secondary layers. The sensors subjected to temperature variation of 80–10 K initially showed a drift from their previous cycles, but it slowly gets stabilized and repeatable after 6th cycle. But the sensors with a chromium buffer layer exhibits non repeatability due to the poor adhesion to indium secondary layer. The temperature sensitivity of the sensors was found to be 34 pm/ K @ 40 K and 13pm/ K at 20 K. With the detection unit of 1 pm resolution an temperature resolution of 0.29 K and 0.76 K respectively can be obtained.

References

- [1] Inaudi D, Glisic B, Scandale W, Garcia Perez J, Billan J, Radaelli S 2001, *Proc. SPIE* **4328**. 79-87
- [2] Fernandez A F, Brichard B, Borgermans P, Berghmans F, Decreton M, Megret P, Blondel M, Delchambre A 2002 *Optical Fiber Sensors Conference Technical Digest*, **Vol.1**. 63-66
- [3] Ramalingam R, Suesser M, Neumann H 2009 *Proceedings OPTO 2009 & IRS² 2009*. 113-118.
- [4] K. Iniewski 2013 *Smart Sensors for Industrial Applications* (Lengmuir: CRC Press)
- [5] Hill K O, Fujii Y, Johnson D C, Kawasaki B S 1978 *Appl. Phys. Lett.*, 1978, **32** 647-9.
- [6] Hill K O, Meltz G 1997 *Journal of Lightwave Technology* **15** 1263-76.
- [7] Kashyap R 1999 *Fiber Bragg Gratings* (Academic Press: San Diego)
- [8] Bharathwaj V, Markan A, Atrey M, Neumann H, Ramalingam R 2014 *Sensor, IEEE* **14834053** 1535-38
- [9] Ramalingam R, Neumann H 2011 *Sensors Journal, IEEE* **11** 1095-1100.
- [10] Ramalingam R, Nast R, Neumann H 2015 *Sensors Journal, IEEE* **15** 2023- 30.
- [11] Ramalingam R, Kläser M, Schneider T, Neumann H 2014 *Sensors Journal, IEEE* **14** 873- 81
- [12] Ramalingam R 2010 *Proc. AIP Conf* **1218** 1197 -1204
- [13] Jicheng L, Neumann H, Ramalingam R 2015 *Cryogenics* **68** 36-43.
- [14] Walstrom P L 1980 *Cryogenics* **20** 509-512
- [15] Ramalingam R and Schwartz M 2012 *AIP Conf. Proc.* **1434** 507
- [16] Ramalingam R 2012 *Proceedings of ICEC 24-ICMC 2012* 43-46
- [17] Ecke W, Latka I, Habisreuther T, Lingertat J 2007 *Proc. SPIE* **6530** 653002
- [18] Xue L, Liu J, Liu Y, Jin L, Gao S, Dong B, Zhao Q, Dong X 2006 *Applied Optics* **45** 8132-35
- [19] Lupi C, Felli F, Brotzu A, Caponero M A, Paolozzi A 2008 *IEEE Sensors Journal* **8** 1299-1304
- [20] Szocs E, Schwager F, Toben M, Brese N 2008 *Proceedings of 2nd Electronics System-Integration Technology Conference* 347-350.